LA-UR-21-26068
Approved for public release; distribution is unlimited.

Title: Symmetry requirements for double shell capsules with aluminum ablators

Author(s): Sacks, Ryan Foster; Loomis, Eric Nicholas; Keiter, Paul Arthur; Merritt, Elizabeth Catherine; Montgomery, David; Sauppe, Joshua Paul; Haines, Brian Michael; Stark, David James; Sagert, Irina; Robey, Harry F. III; Palaniyappan, Sasikumar; Morrow, Tana; Finnegan, Sean Michael; Kline, John L.; Batha, Steven H.

Intended for: Report

Issued: 2021-06-28

Symmetry requirements for double shell capsules with aluminum ablators

Ryan Sacks,* Eric Loomis, Paul Keiter, Elizabeth Merritt, David Montgomery, Joshua Sauppe, Brian Haines, David Stark, Irina Sagert, Harry Robey, Sasikumar Palaniyappan, Tana Morrow, Sean Finnegan, John Kline, and Steve Batha
Los Alamos National Laboratory, Los Alamos, NM 87545 USA
(Dated: June 28, 2021)

Double shell targets present a promising avenue to obtain robust neutron yield on current laser facilities. The nature of the target, like current single shell designs, requires a symmetric implosion of an outer ablator to obtain a symmetric fuel volume that will lead to alpha heating and thermonuclear burn. Due to using aluminum as an ablator material and requiring different convergence than single shell symmetry studies at various energies are required. This paper moves forward from previous experiments conducted at 1MJ to show implosion symmetry at 1.25 and 1.5MJ. Symmetry in these experiments is sufficient to merit experiments using double shells to study the platform further. Additional studies are carried out on the outer shell symmetry impacts, showing that mitigating mode growth on the outer ablator is of great importance.

I. INTRODUCTION

Progress toward robust burn on the National Ignition Facility (NIF) [1] has been made through a number of novel ideas when compared to the initial point design used during the National Ignition Campaign [2, 3]. These advancements have come through the investigation of the deleterious effects of low mode instability growth[4], tent perturbations, and the fill tube[5]. Changes in the design include a reduction in the number of launched shocks from four to three [6] and possibly to two[7], a reduction in the thickness of the support tent and the diameter of the fill tube[5], and a change toward more stable ablator materials including high density carbon[8–11] and beryllium[11–15]. However, all of these changes still rely on the concept of hot-spot ignition [2, 3, 16, 17]. While current results show alpha-heating of the DT fuel[18], there is yet to be evidence of a propagating burn wave that will result in high yield targets showing robust burn.

In contrast to hotspot ignition proposals, double shell target designs [19–22](See Figure 1) rely on two physical phenomenon to reach robust burn; volumetric ignition and radiation trapping. By having a higher initial density of DT fuel, at a liquid density of 0.2g/cc instead of an ice layer with a low density DT gas fill, higher values of rhoR can be achieved at a lower convergence. This technique uses the entire volume of fuel to initiate burn instead of a core hotspot. In addition, the compression and ionization of the fuel, which in turn releases radiation, is trapped in the fuel by the high-Z inner shell. As there are fewer radiative loss mechanisms due to this trapping, a lower initial ion temperature is required in order to obtain robust burn. By virtue of this lower initial temperature and lower required convergence ratio, an overall lower implosion velocity of the inner shell is required when compared to single shell designs. No design is without its own obstacles, double shells included. Due to the complex design requiring concentric shells, target fabrication is a challenge.

In moving forward with the double shell platform, qualification of multiple physics questions is required. Previously at low laser energies [23] both the shape of the outer shell and its transfer to an inner shell are benchmarked against simulation. While useful, this was at energies around 1MJ on the NIF, while the point design for robust yield requires a laser energy of 1.5MJ . Due to the nature of the target, using an aluminum ablator instead of the already tested high density carbon[8–11] CH plastic [2, 3, 5, 6], or beryllium [11–15], testing is needed investigate laser coupling, back scatter, and ablation rate. This requires a step up in laser energy from 1MJ to 1.5MJ. Doing so allows for an investigation of how the outer ablator shape changes as laser power is increased. This is of importance as a symmetric outer shell implosion is needed so that low modes are not imprinted onto the inner shell, causing a deleterious impact on capsule performance. The aim of this paper is that

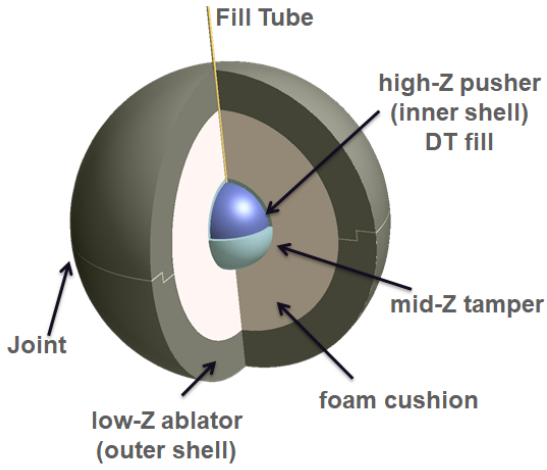

FIG. 1. 3-D model of a double shell target. Aspects of interest for the target concept include the impact of the fill tube, impact of the joint, and impact of surface roughness at each of the material interfaces.

* rsacks@lanl.gov

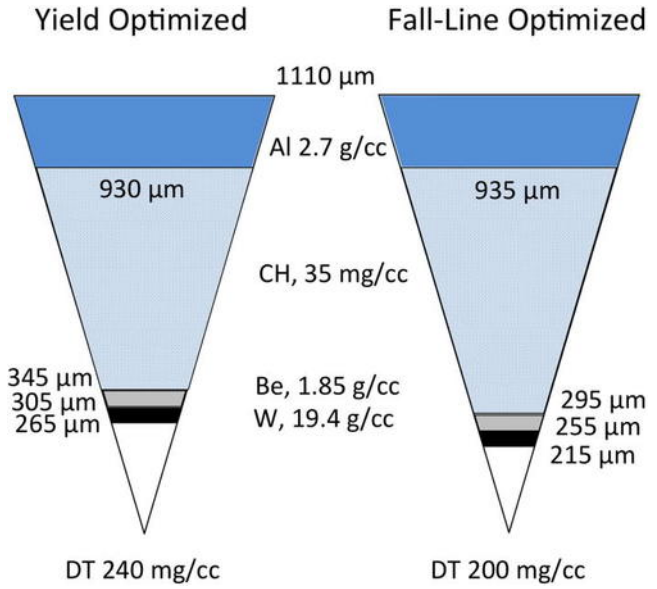

FIG. 2. Pie diagrams for a yield optimized capsule with greater inner shell convergence, and a fall-line optimized design which is more robust against hydrodynamic instabilities and mix. The fall-line design trades off convergence and yield for a more stable implosion. Figure courtesy of David Montgomery from reference [22].

to show that as laser power is increased, simulation results concur with the experimental results to the degree expected, and that the shape is appropriate to continue forward with investigations of other physics aspects of the double shell platform. The next section of the paper will demonstrate ways of controlling the shape with changes to the laser pulse and the impact of initial low mode shape from target construction. The third section of the paper will demonstrate simulation agreement with experiments.

II. SIMULATIONS OF DOUBLE SHELL SHAPE

The main design of the double shell platform (See Figure 2) is used as a base line for the setup of the experiments used. This design is a fall-line optimized design for use with a 1.5MJ reverse ramp laser pulse. The fall line is defined as taking a line of constant velocity at the minimum fuel radius and extrapolating it zero radius, see the paper by Welser-Sherrill et al. for more detail [24]. Comparing that intercept to the time of maximum neutron production gives a value of the fall, and maximizing this value leads to a fall-line optimized design. Outer shell experiments using only the aluminum ablator are selected to show control and symmetry of the imploding ablator. All experiments were designed using Lawrence Livermore National Laboratory's HYDRA code[25]. The experiments are to examine the shape of the outer ablator as it implodes in towards an inner radius of 300 μm. This is measured experimentally using a 2 dimensional convergent ablator setup (commonly referred to as a '2DConA')[26]. We use near vacuum [27, 28] hohlraums to minimize laser light scattering back out of the hohlraum. Using the laser profile in figure 3 simulations of the double shell capsules show more of a P4 depression at 45 degrees, but also a P2 asymmetry that needs to be controlled. This needs to be controlled, as having an asymmetric implosion impacts overall performance of the capsule. A higher overall foam pressure is desirable, as that will lead to more energy being imparted to the inner shell, giving more overall yield. In figure 4 we show that the fall-line design has about a factor of two more foam pressure, reinforcing our choice of this design. The fall-line optimized design shown in 2 is selected over a yield optimized design, also shown in 2, as those optimizations are done using 1-D simulations. By utilizing 2-D simulations that allow for imperfections in the drive to manifest, changes in the pressure profile present in the foam show that the fall-line design is a more robust option than the yield optimization. A design that is insensitive to low mode shape is desirable as other imperfections in the capsule will degrade the performance, but with a higher base line to work from, the impact of those imperfections will be lessened. The choice of the fall-line optimized design is based on several factors. These are explained in the paper by Montgomery et al. [22], but come down to the fact that the fall line optimized design has a higher specific fuel internal energy, and the simulated 2-D yield versus the 1-D no mix yield for the fall-line design is 70% compared to the yield optimized at only 2%.

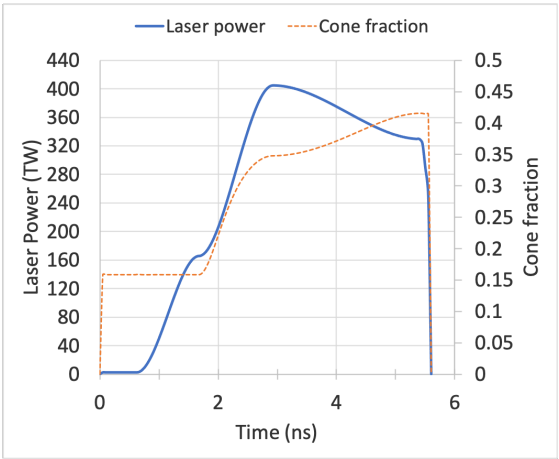

FIG. 3. Schematic of the baseline laser power profile and time-dependent cone fraction used in the parameter studying assessing the impact of initial Pn modes on double shell implosion shape.

Studying shape control is simplest with single modes and multiple parameter changes in the design. By imposing a single mode onto the capsule and varying different parameters, ways to mitigate deformation of the capsule can be investigated. There are several parameters that deserve attention: outer cone pointing, hohlraum gas fill, initial mode amplitude, and adjustment of cone fractions.

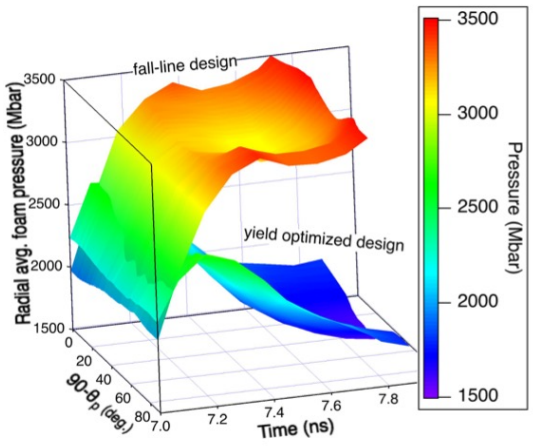

FIG. 4. Comparison of the average foam pressure of two designs for double shells. The fall line design shows a more robust average foam pressure than the yield design, making it more attractive.

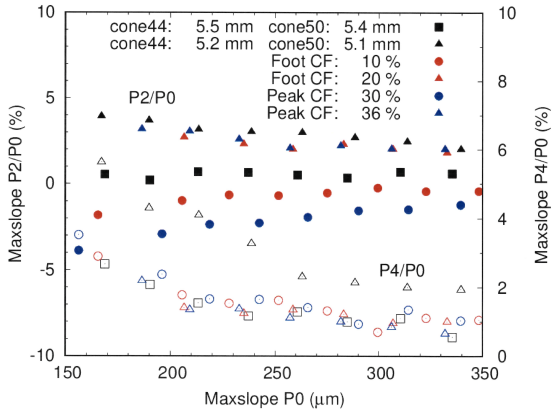

FIG. 5. Impact of cone fraction and outer cone pointing on the P2 and P4 asymmetries. In general increasing the cone fraction pushes the P2/P0 (solid symbols) in a positive (prolate) direction. Moving the outer cones further from the LEH moves both the P2/P0 and P4/P0 (open symbols) in a negative (square) direction. Changes to the cone fraction have a negligible impact on P4/P0.

Using integrated capsule-hohlraum HYDRA simulations with laser ray tracing, variations on these parameters can be studied, and their impact on the shape of the outer shell of the capsule assessed. By varying the outer cone pointing by $300\mu m$ and adjusting the energy balance between the inner and outer cones (also called cone fraction), HYDRA simulations suggest that the P2 and P4 shape of the outer ablator can be controlled. As is shown in figure 5 there are two main ways of adjusting the shape of the outer ablator. By adjusting the cone fraction, either at the peak or during the foot of the pulse, the P2/P0 can be changed. Increasing the cone fraction adjusts the P2/P0 fraction in the positive (prolate) direction, yet it has a negligible impact on the P4/P0 shape. In order to adjust the P4 the position of the outer, specifically the 44.5 and 50 degree, cones must be moved further from the LEH. Doing this pushes the P4/P0 shape in the negative (square) direction. This study is very useful as it gives a general idea of what steps need to be taken in order to obtain a more symmetric outer shell implosion.

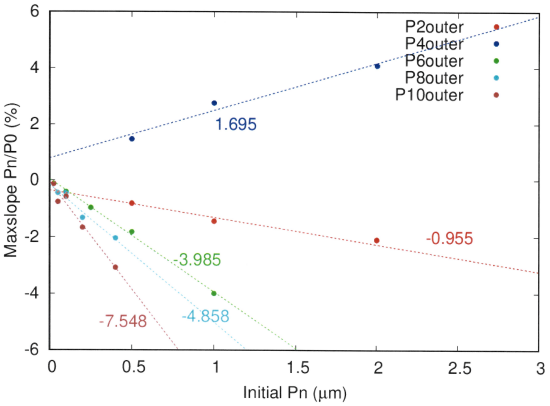

FIG. 6. Impact of increasing initial Pn shape on the outer part of the ablator. Fit lines with slope show how impactful each even mode is with increasing initial amplitude.

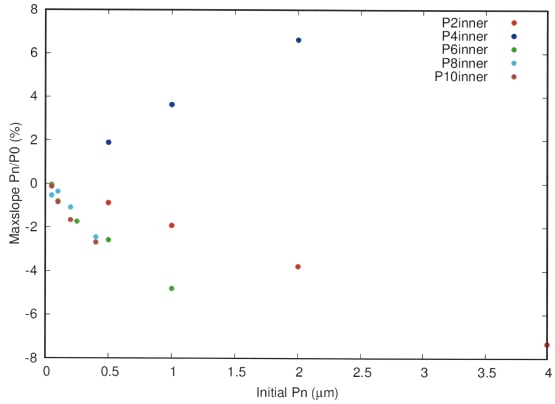

FIG. 7. Impact of increasing initial Pn shape on the inner part of the ablator.

Adjusting laser parameters is not the only way to introduce or mitigate asymmetry on the capsule. Machining can leave an initial perturbation on the capsule which can propagate inward as the implosion progresses. These imprinted modes on the outer shell arise from diamond turning machining of the aluminum hemispheres that make up the outer ablator. This is significantly different from a sputter coated shell, which would not have evidence of the machining, but instead have high mode surface irregularities arising from the mandrel. Machining allows for extremely smooth surfaces, but controlling the concentricity of outer and inner surfaces is extremely difficult. Machining can also lead to a joint gap distance in the pole-to-pole direction which is different than across the equator by several microns. Machining two separate hemispheres also requires the use of machines to press the two parts together to create a single sphere, which can lead to deformation of the material where the parts

are being held and along the joint. Using the pulse shape shown in figure 3, a study of these initial imprinted modes can be seen in figures 6 and 7, which is useful as not all modes are created equally. By applying an initial perturbation on the outer edge of the ablator and then imploding the shell, the different growth can be seen. The values shown in figure 6 are taken at an implosion radius of $300\mu m$, as this is where shell collision between the inner and outer shell occurs. It is not always the case of a higher mode leading to more imprinting, as the figure shows that there is a monotonically increasing impact with increasing mode number. A higher initial mode value for any mode has a larger impact, and the higher the mode number, the impact becomes larger in amplitude. Applying the initial perturbations on the inner portion of the ablator as in figure 7 also has a different imprint than the other (outer) surface shown in figure 6. For the inner ablator perturbations the impact of the perturbation is more pronounced, leading to a higher amount of imprinting than when the perturbation is on the outer edge. This is due to several factors, including the lack of any ablative stabilization, and the lack of any higher density aluminum that can prevent deformation of the ablator as the shock propagates through the material.

III. SHAPE EXPERIMENTS ON NIF AND POST SHOT SIMULATIONS

This shape study will focus on 4 separate NIF experiments; N180321, N180522, N181125, and N190520. All of these experiments measured the time dependent outer shell shape using the 2D ConA platform[26]. The laser energy, hohlraum specifications, and outer ablator thickness are presented in table I. The first shot, N180321 is examined and the pulse shapes of subsequent shots are derived from it. For more information on 1MJ shape see the paper by Merritt et. al. [23]. N180522 and N181125 are examined as they are an upgrade from 1MJ to 1.25MJ and show that by changing the cone fraction and pulse shpaethe symmetry of the capsule is controllable. The fourth shot (N190520) utilizes the design energy of 1.5 MJ. All the shots were analyzed with HYDRA using the as fielded capsule, hohlraum, and laser specifications based on the paper by Jones et al. [29]. For a list of options in the code used for the post-shot simulations see table II. The main differences in the shots are shown in figures of the pulses at the start of each shot's subsection, with the higher energy shots having a higher temperature in the hohlraum, and the cone fractions changing in order to control symmetry. All shots are conducted with what is known as a reverse ramp pulse, which as figure 8 shows has a large initial ramp to full laser power, then trails off until the lasers shut off at 4.75-5.6ns, with increasing pulse length corresponding with increasing energy.

Shot Name	**Laser Energy**	**Hohlraum Size**	**Capsule thickness**
N180321	1.0 MJ	5.75mm dia 10.13mm length	$106\mu m$
N180522	1.25 MJ	5.75mm dia, 10.13mm length	$120\mu m$
N181125	1.25 MJ	5.75mm dia, 10.13mm length	$120\mu m$
N190520	1.5 MJ	5.75mm dia, 10.13mm length	$128\mu m$

TABLE I. List of shot and hohlraum information.

HYDRA Parameter	**Parameter Setting**
Au wall zoning	40 Angstrom first zone
DCA opacity	2017, 79e
Photon Resolution	85 groups
Laser Rays	600 traces
Power Multiplier	0.94
Angular zoning	1 degree per zone

TABLE II. HYDRA options used for the simulations.

III.1. 1MJ Shot N180321

Shot N180321 is a 1MJ laser pulse (shown in figures 8 and 9) inside of a nominal 5.75mm diameter hohlraum. The capsule thickness is $106\mu m$ to be transmissive enough at a radius of $300\mu m$. Values for for the trajectory and shape of the experiment vs the post shot simulation can be found in figures 10 and 11. This data shows that for a 1MJ pulse, the shape of the experiment can be simulated by HYDRA nearly within the expected error, and going through the middle of the data. This is the case for the P0 trajectory and the P2 shape. The P4 shape is slightly over predicted by the simulation, however this is an acceptable error as that means the experiment performs better than expected. With the confidence that a lower power 1MJ shot can be modeled, increasing the power is the next step.

III.2. 1.25MJ Shots N180522 and N181125

Taking an incremental step in power is a reasonable iteration on the design, as ensuring that increases in power do not significantly impact shape, and that the adjustments used previously to change shape are still appropriate. Both shots N180522 and N181125 are experiments conducted at 1.25MJ. The main difference between the two of them is that the cone fractions are adjusted between them in order to attempt to control the P2 shape, as shown in figures 8 and 9. The P0 trajectories, shown in figures 12 and 13, for each experiment the simulation have an error when attempting to recreate the experimental data. The source of this discrepency is still under

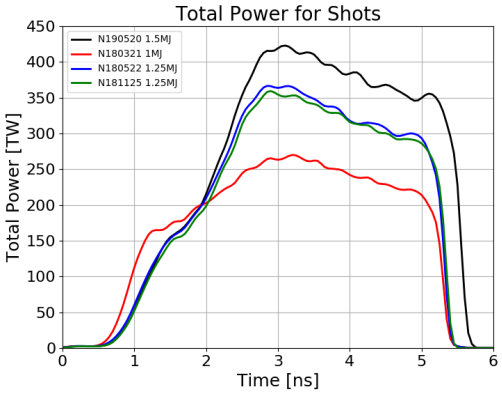

FIG. 8. Laser power for each of the four experiments. The difference in laser energy between N180522 and N181125 is less than 30kJ.

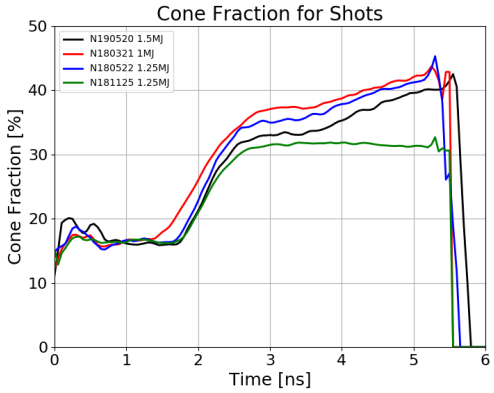

FIG. 9. Cone fractions used in each experiment. The change in late time cone fraction between N180522 and N181125 is to demonstrate a change in the P2 shape.

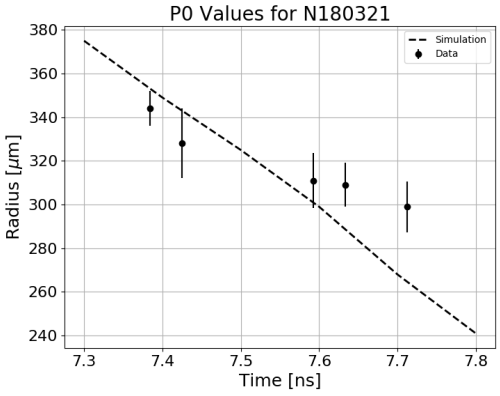

FIG. 10. P0 trajectory of shot N180321

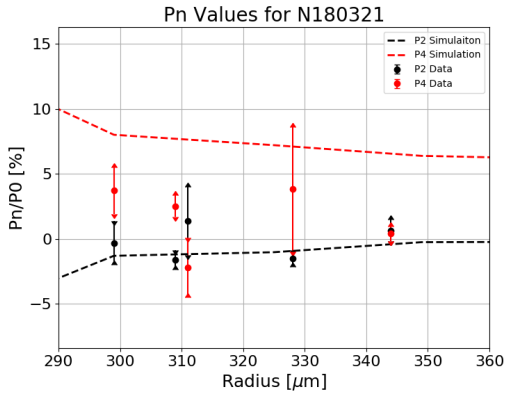

FIG. 11. P2 shape of shot N180321

investigation. By examining the plots shown in figures 14 and 15, both the data and the simulation show that by adjusting the cone fractions in the shot, the P2 shape is improved. The figures further show that as suggested by the previous simulation study, the P4 shape can be impacted by changes in the cone fraction, but they are not as significant as the changes in the P2. Thus changes in the beam pointing in relation to the laser entrance hole are the more effective way of altering the P4 shape.

III.3. 1.5 MJ Shot N190520

The last shot to be discussed in this paper is the first 1.5MJ (pulse shape shown in figures 8 and 9) shot with an aluminum ablator in a standard 5.75mm hohlraum, N190520. This experiment shows that by using the established methods to adjust shape, both in previous shots of increasing power, and through a simulation study of the parameter space, reasonable predictions of the trajectory and shape can be made. The trajectory data shown in figure 16 is matched nearly exactly within the error bars except at late time and small radius. The same is true of the low mode shape in figure 17, with the only discrepancy being at small radius. The results of these experiments and simulations show that while there is work to be done to improve the overall shape of the implosions, the simulation can be used as an accurate barometer of the experiment. Using techniques described previously, simulations can be done to improve the shape and the experiments will likely bear out those changes.

IV. SUMMARY

Symmetry for double shells, like many other targets on the NIF that seek any degree of thermonuclear burn, are sensitive to shape. Controlling the low mode shape is incredibly important for double shells. By examining both a fall line optimized design and a yield optimized design, a selection is made to use the fall line optimized design due to its inherent robustness to ward off deleterious effects from low mode shape. This is due to maintaining a higher foam pressure, which resists imprinting onto the inner shell. This gives more robustness to any shape issues that may arise from the laser pulse and hohlraum. Studying the design in HYDRA shows that low mode

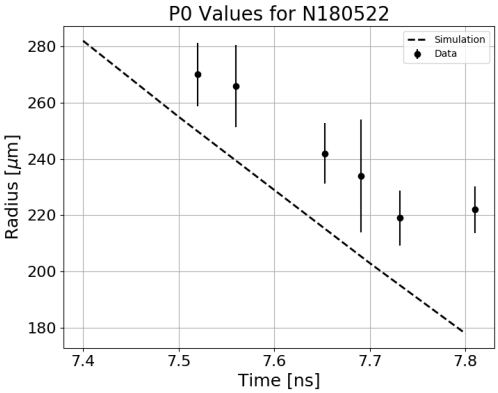

FIG. 12. P0 trajectory of shot N180522

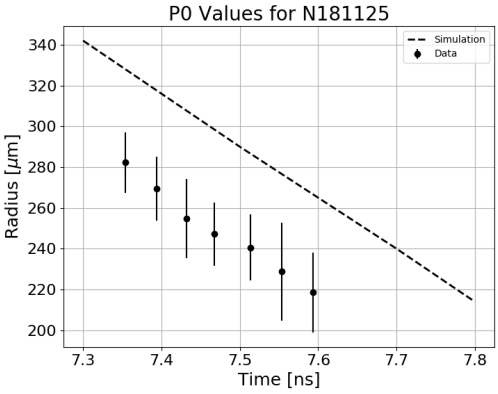

FIG. 13. P0 trajectory of shot N181125

shape is an area of concern as the even modes 2-10 do cause shape issues from the outer ablator which can be transferred to the inner shell. Simulations suggest that these issues can be mitigated by adjusting the cone fraction used in the laser pulse and by adjusting the pointing of the outer cone beams with regard to the leaser entrance hole. The predictability of this simulation study is put into practice in 4 shots of increasing power on the NIF using aluminum ablators. These experiments show simulations are able to predict the low mode P2 and P4 shape of the implosions at larger radii that correspond to the impact of the outer shell onto the inner shell at roughly $300\mu m$.The P0 trajectory of the outer shell is matched within the error bars for the 1MJ and 1.5MJ shots, while the 1.25MJ shots still have slight discrepancies that are still under investigation. Due to the desire to continue forward 1.5MJ experiments as that is the energy for the fall line optimized design, the HYDRA parameters, specifically the power multiplier of 0.94 were chosen as they match the 1.5MJ shot. That power multiplier may need to be adjusted for the 1.25MJ shots in order to create a more accurate model.

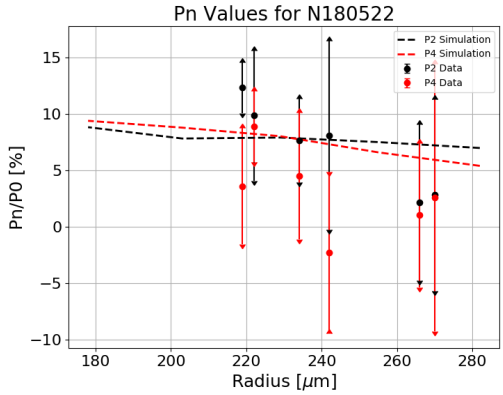

FIG. 14. Pn shape of shot N180522

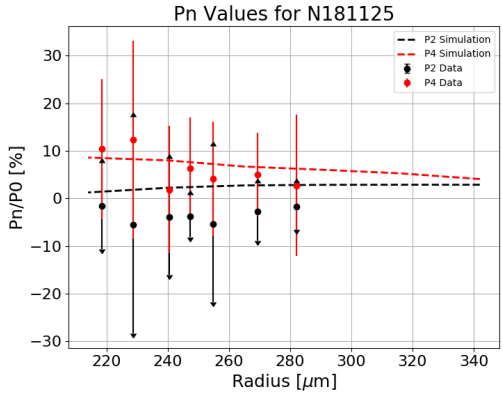

FIG. 15. Pn shape of shot N181125

V. ACKNOWLEDGEMENTS

The Los Alamos Double Shell team would like to thank the following Lawrence Livermore National Laboratory staff: Oggie Jones, Scott Sepke, and Mehul Patel for their assistance in running simulations. Shahab Khan for help in analyzing the 2D ConA experiments. And Peter Amendt, Robert Tipton, Vladimir Smalyuk, and Yuan Ping for previous conversations on double shell physics issues. Release number LA-UR-XXXXXX.

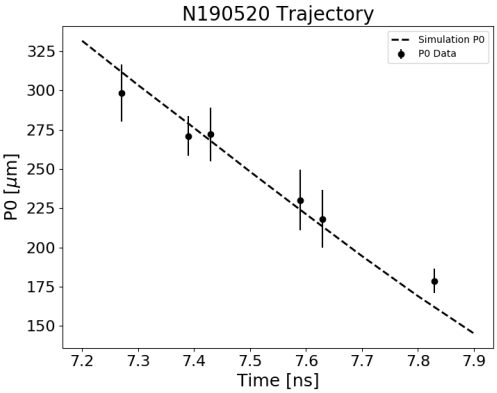

FIG. 16. P0 trajectory of shot N190520

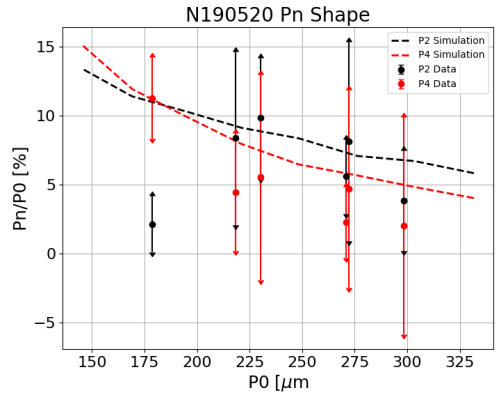

FIG. 17. Pn shape of shot N190520

REFERENCES

[1] E. I. Moses and C. R. Wuest. *Fusion Science and Technology*, 43(3):420, 2003.

[2] J. Lindl, O. Landen, J. Edwards, E. Moses, and NIC Team. *Physics of Plasmas*, 21:020501, 2014.

[3] S. W. Haan, J. D. Lindl, D. A. Callahan, D. S. Clark, J. D. Salmonson, B. A. Hammel, L. J. Atherton, R. C. Cook, M. J. Edwards, S. Glenzer, A. V. Hamza, S. P. Hatchett, M. C. Herrmann, D. E. Hinkel, D. D. Ho, H. Huang, O. S. Jones, J. Kline, G. Kyrala, O. L. Landen, B. J. MacGowan, M. M. Marinak, D. D. Meyerhofer, J. L. Milovich, K. A. Moreno, E. I. Moses, D. H. Munro, A. Nikroo, R. E. Olson, K. Peterson, S. M. Pollaine, J. E. Ralph, H. F. Robey, B. K. Spears, P. T. Springer, L. J. Suter, C. A. Thomas, R. P. Town, and R. Vesey. *Physics of Plasmas*, 18:051001, 2011.

[4] G. Kyrala, N. Delamater, D. Wilson, J. Guzik, D. Haynes, M. Gunderson, K. Klare, R. Watt, W. Wood, and W. Varnum. *Laser Particle Beams*, 23:187, 2005.

[5] D. S. Clark, M. M. Marinak, C. R. Weber, D. C. Eder, S. W. Haan, B. A. Hammel, D. E. Hinkel, O. S. Jones, J. L. Milovich, P. K. Patel, H. F. Robey, J. D. Salmonson, S. M. Sepke, and C. A. Thomas. *Physics of Plasmas*, 22:022703, 2015.

[6] O. A. Hurricane, D. A. Callahan, D. T. Casey, E. L. Dewald, T. R. Dittrich, T. Doppner, M. A. Barrios Garcia, D. E. Hinkel, L. F. Berzak Hopkins, P. Kervin, J. L. Kline, S. Le Pape, T. Ma, A. G. MacPhee, J. L. Milovich, J. Moody, A. E. Pak, P. K. Patel, H. S. Park, B. A. Remington, H. F. Robey, J. D. Salmonson, P. T. Springer, R. Tommasini, L. R. Benedetti, J. A. Caggiano, P. Celliers, C. Cerjan, R. Dylla-Spears, D. Edgell, M. J. Edwards, D. Fittinghoff, G. P. Grim, N. Guler, N. Izumi, J. A. Frenje, M. Gatu Johnson, S. Haan, R. Hatarik, H. Herrmann, S. Khan, J. Knauer, B. J. Kozioziemski, A. L. Kritcher, G. Kyrala, S. A. Maclaren, F. E. Merrill, P. Michel, J. Ralph, J. S. Ross, J. R. Rygg, M. B. Schneider, B. K. Spears, K. Widmann, and C. B. Yeamans. *Physics of Plasmas*, 21:056314, 2014.

[7] S. F. Khan, S. A. MacLaren, J. D. Salmonson an T. Ma, G. A. Kyrala, J. E. Pino, J. R. Rygg, J. E. Field, R. Tommasini, J. E. Ralph, D. P. Turnbull, A. J. Mackinnon, K. L. backer, L. R. Benedetti, D. K. Bradley, P. M. Celliers, E. L. Dewald, T. R. Dittrich, L. Berzak Hopkins, N. Izumi, M. L. Kervin, J.L. Kline, S. R. Nagel, A. Pak, and R. E. Tipton. *Physics of Plasmas*, 23:042708, 2016.

[8] K. L. Baker, C. A. Thomas, D. T. Casey, S. Khan, B. K. Spears, R. Nora, T. Woods, J. L. Milovich, R. L. Berger, D. Strozzi, D. Clark, M Hohenberger, O. A. Hurricane D. A. Callahan, O. L. Landen, B. Bachmann, R. Benedetti, R. Bionta, P. M. Celliers, D. Fittinghoff, C. Goyon, G. Grim, R. Hatarik, N. Izumi, M. Gatu Johnson, G. Kyrala, T. Ma, M Millot, S. R. Nagel, A. Pak, P. K. Patel, D. Turnbull, P. L. Volegov, and C. Yeamans. *Physical Review Letters*, 121:135001, 2018.

[9] S. Le Pape, L. F. Berzak Hopkins, L. Divol, A. Pak, E. L. Dewald, S. Bhandarkar, L. R. Bennedetti, T. Bunn, J. Biener, J. Crippen, D. Casey, D. Edgell, D. N. Fittinghoff, M. Gatu-Johnson, C. Goyon, S. Haan, R. Hatarik, M. Havre, D. D-M. Ho, N. Izumi, J. Jaquez, S. F. Khan, G. A. Kyrala, T. Ma, A. J. Mackinnon, A. G. MacPhee, B. J. MacGowan, N. B. Meezan, J. Milovich, M. Millot, P. Michel, S. R. Nagel, A. Nikroo, P. Patel, J. Ralph, J. S. Ross, N. G. Rice, D. Strozzi, M. Stadermann, P. Volegov, C. Yeamans, C. Weber, C. Wild, D. Callahand, and O. A. Hurricane. *Physical Review Letters*, 120:245003, 2018.

[10] D. D.M. Ho, S. W. Haan, J. D. Salmonson, D. S. Clark, J. D. Lindl, J. L. Milovich, C. A. Thomas, L. F. Berzak Hopkins, and N. B. Meezan. *Journal of Physics Conference Series*, 717:012023, 2016.

[11] D. S. Clark, A. L. Kritcher, S. A. Yi, A. B. Zylstra, S. W. Haan, and C. R. Weber. *Physics of Plasmas*, 25:032703, 2018.

[12] J. L. Kline, S. A. Yi, A. N. Simakov, R. E. Olson, D. C. Wilson, G. A. Kyrala, T. S. Perry, S. H. Batha, A. B. Zylstra, E. L. Dewald, R. Tommasini, J. E. Ralph, D. J. Strozzi, A. G. MacPhee, D. A. Callahan, D. E. Hinkel, O. A. Hurricane, J. L. Milovich, J. R. Rygg, S. F. Khan, S. W. Haan, P. M. Celliers, D. S. Clark, B. A. Hammel, B. Kozioziemski, M. B. Schneider, M. M. Marinak, H. G. Rinderknecht, H. F. Robey, J. D. Salmonson, P. K. Patel, T. Ma, M. J. Edwards, M. Stadermann, S. Baxamusa, C. Alford, M. Wang, A. Nikroo, N. Rice, D. Hoover, K. P. Youngblood, H. Xu, H. Huang, and H. Sio. *Physics of Plasmas*, 23:056310, 2016.

[13] D. C. Wilson, S. A. Yi, A. N. Simakov, J. L. Kline, G. A. Kyrala, E. L. Dewald, R. Tommasini, J. E. Ralph, R. E. Olson, D. J. Strozzi, P. M. Celliers, M. B. Schneider, A. G. MacPhee, A. B. Zylstra, D. A. Callahan, O. A. Hurricane, J. L. Milovich, D. E. Hinkel, J. R. Rygg, H. G. Rinderknecht, H. Sio, T. S. Perry, and S. Batha. *Journal of Physics: Conference Series*, 717:012058, 2016.

[14] A. B. Zylstra, S. A. Yi, S. MacLaren, J. Kline, G. Kyrala, J. E. Ralph, J. Bae, S. Batha, D. Callahan, K. Flippo, H. Huang, O. Hurricane, S. F. Khan, N. Kabadi, C. Kong, L. B. Kot, E. N. Loomis, L. P. Masse, M. Millot, A. Moore, A. Nikroo, T. S. Perry, N. Rice, J. Salmonson, R. Shah, H. Sio, M. Stadermann, D. J. Strozzi, R. Tipton, and H. Xu. *Physics of Plasmas*, 25:102704, 2018.

[15] A. N. Simakov, D. C. Wilson, S. A. Yi, E. N. Loomis, J. L. Kline, G. A. Kyrala, A. B. Zylstra, E. L. Dewald, R. Tommasini, J. E. Ralph D. J. Strozzi, A. G. MacPhee, J. L. Milovich, J. R. Rygg, S. F. Khan, T. Ma, L. C. Jarrott, S. W. Haan, P. M. Celliers, M. M Marinak, H. G. Rinderknecht, H. F. Robey, J. D. Salmonson, M. Stadermann, S. Baxamusa, C. Alford, Y. Wang, A. Nikroo, N. Rice, C. Kong, J. Jaquez, M. Mauldin, K. P. Youngblood, H. Xu, H. Huang, and H. Sio. *Physics of Plasmas*, 24:052704, 2017.

[16] Stefano Atzeni and Jurgen Meyer ter vehn. *The Physics of Inertial Fusion*. Oxford University Press, 2004,2009.

[17] R Paul Drake. *High Energy Density Physics*. Springer International Publishing, 2006,2018.

[18] O. A. Hurricane, D. A. Callahan, D. T. Casey, P. M. Celliers, C. Cerjan, E. L. Dewald, T. R. Dittrich, T. Doppner, D. E. Hinkel, L. F. Berzak Hopkins, J. L. Kline, S. Le Pape, T. Ma, A. G. MacPhee, J. L. Milovich,

A. Pak, H. S. Park, P. K. Patel, B. A. Remington, J. D. Salmonson, P. T. Springer, and R. Tommasini. *Nature*, 506:343, 2014.

[19] J. L. Milovich, P. Amendt, M. Marinak, and H. Robey. *Physics of Plasmas*, 11:1552, 2004.

[20] W. S. Varnum, N. D. Delamater, S. Evans, P. L. Gobby, J. E. Moore, J. M. Wallace, and R. G. Watt. *Physical Review Letters*, 84:5153, 2000.

[21] P. Amendt, J. D. Colvin, R. E. Tipton, D. E. Hinkel, M. J. Edwards, O. L. Landen, J. D. Ramshaw, L. J. Suter, W. S. Varnum, and R. G. Watt. *Physics of Plasmas*, 9:2221, 2002.

[22] D. S. Montgomery, W. S. Daughton, B. J. Albright, A. N. Simakov, D. C. Wilson, E. S. Dodd, R. C. Rirkpatrick, R. G. Watt, M. A. Gunderson, E. N. Loomis, E. C. Loomis, T. Cardenas, P. Amendt, J. L. Milovich, H. F. Robey, R. E. Tipton, and M. D. Rosen. *Physics of Plasmas*, 25:092706, 2018.

[23] E. C. Merritt, J. P. Sauppe, E. N. Loomis, T. Cardenas, D. S. Montgomery, W. S. Daughton, D. C. Wilson, J. L. Kline, S. F. Khan, M. Schoff, M. Hoppe, F. Fierro, R. B. Randolph, B. Patterson, L. Kuettner, R. F. Sacks, E. S. Dodd, W. C. Wan, S. Palaniyappan, S. H. Batha, P. A. Keiter, J. R. Rygg, V. Smalyuk, Y. Ping, and P. Amendt. *Physics of Plasmas*, 26:052702, 2019.

[24] L. Welser-Sherrill, R. C. Mancini, D. A. Haynes, S. W. Haan, I. E. Golovkin, J. J. MacFarlane, P. B. Radha, J. A. Delettrez, S. P. Regan, J. A. Koch, N. Izumi, R. Tommasini, and V. A. Smalyuk. *Physics of Plasmas*, 14:072705, 2007.

[25] M. M. Marinak, G. D. Kerbel, N. A. Gentile, O. Jones, D. Munro, S. Pollaine, T. R. Dittrich, and S. W. Haan. *Physics of Plasmas*, 8:2275, 2001.

[26] J. R. Rygg, O. S. Jones, J. E. Field, M. A. Barrios, L. R. Benedetti, G. Collins, D. C. Eder, M. J. Edwards, J. L. Kline, J. J. Kroll, O. L. Landen, T. Ma, A. Pak, J. L. Peterson, K. Raman, R. P. J. Town, and D. K. Bradley. *Physical Review Letters*, 112:195001, 2014.

[27] L. F. Berzak Hopkins, N. B. Meezan, S. Le Pape, L. Divol, A. J. Mackinnon, D. D. Ho, M. Hohenberger, O. S. Jones, G. Kyrala, J. L. Milovich, A. Pak, J. E. Ralph, J. S. Ross, L. R. Benedetti, J. Biener, R. Bionta, E. Bond, D. Bradley, J. Caggiano, D. Callahan, C. Cerjan, J. Church, D. Clark, T. Doppner, R. Dylla-Spears, M. Eckart, D. Edgell, J. Field, D. N. Fittinghoff, M. G. Johnson, G. Grim, N. Guler, S. Haan an dA. Hamza, E. P. Hartouni, R. Hatarik, H. Herrmann, D. Hinkel, D.. Hoover, H. Huang, N. Izumi, S. Khan, B. Kozioziemski, J. Kroll, T. Ma, A. MacPhee, J. McNaney, F. Merrill, J. Moody, A. Nikroo, P. Patel, H. F. Robey, J. R. Rygg, J. Sater, D. Sayre, M Schneider, S. Sepke, M. Stadermann, W. Stoeffl, C. Thomas, R. P. J. Town, P. L. Volegov, C. Wild, C. Wilde, E. Woerner, C. Yeamans, B. Yoxall, J. Kilkenny, O. L. Landen, W. Hsing, and M. J. Edwards. *Physical Review Letters*, 114:175001, 2015.

[28] L. F. Berzak Hopkins, S. Le Pape, L. Divol, N. B. Meezan, A. J. Mackinnon, D. D. Ho, O. S. Jones, S. Khan, J. L. Milovich, J. S. Ross, P. Amendt, D. Casey, P. M. Celliers, A. Pak, J. L. Peterson, J. Ralph, and J. R. Rygg. *Physics of Plasmas*, 22:056318, 2015.

[29] O. S. Jones, L. J. Suter, H. A. Scott, M. A. Barrios, W. A. Farmer, S. B. Hansen, D. A. Liedahl, C. W. Mauche, A. S. Moore, M. D. Rosen, J. D. Salmonson, D. J. Strozzi, C. A. Thomas, and D. P. Turnbull. *Physics of Plasmas*, 24:056312, 2017.